1 *Enterococcus faecalis* strains with compromised CRISPR-Cas defense emerge under antibiotic

2 selection for a CRISPR-targeted plasmid

3

4 Wenwen Huo[ab], Valerie J. Price[ab], Ardalan Sharifi[a], Michael Q. Zhang[a], and Kelli L. Palmer[a]*

5

6 Department of Biological Sciences, The University of Texas at Dallas, Richardson, Texas, USA[a]

7 [b]These authors contributed equally

8 *Corresponding author

9 E-mail: kelli.palmer@utdallas.edu (KLP)

Abstract

Enterococcus faecalis is a Gram-positive bacterium that natively colonizes the human gastrointestinal tract and opportunistically causes life-threatening infections. Multidrug-resistant (MDR) *E. faecalis* strains have emerged that are replete with mobile genetic elements (MGEs). Non-MDR *E. faecalis* strains frequently possess CRISPR-Cas systems, which reduce the frequency of mobile genetic element (MGE) acquisition. We demonstrated in previous studies that *E. faecalis* populations can transiently maintain both a functional CRISPR-Cas system and a CRISPR-Cas target. In this study, we used serial passage and deep sequencing to analyze these populations. In the presence of antibiotic selection for the plasmid, mutants with compromised CRISPR-Cas defense and enhanced ability to acquire a second antibiotic resistance plasmid emerged. Conversely, in the absence of selection, the plasmid was lost from wild-type *E. faecalis* populations, but not *E. faecalis* populations that lacked the *cas9* gene. Our results indicate that *E. faecalis* CRISPR-Cas can become compromised under antibiotic selection, generating populations with enhanced abilities to undergo horizontal gene transfer.

Importance

Enterococcus faecalis is a leading cause of hospital-acquired infections and disseminator of antibiotic resistance plasmids among Gram-positive bacteria. We have previously shown that *E. faecalis* strains with an active CRISPR-Cas system can prevent plasmid acquisition and thus limit the transmission of antibiotic resistance determinants. Yet, CRISPR-Cas was not a perfect barrier. In this study, we observed populations of *E. faecalis* with transient co-existence of CRISPR-Cas and one of its plasmid targets. Our experimental data demonstrate that antibiotic selection results in compromised *E. faecalis* CRISPR-Cas function, thereby facilitating the acquisition of additional resistance plasmids by *E. faecalis*.

Introduction

Enterococcus faecalis is a Gram-positive bacterium that natively colonizes the human gastrointestinal tract and opportunistically causes life-threatening infections (1-4). Antibiotic resistance is a major concern for treatment of these infections. *E. faecalis* can acquire antibiotic resistance through horizontal gene transfer (HGT), mediated primarily by plasmids, transposons, and integrative conjugative elements (5-7). One of the most clinically relevant forms of HGT in *E. faecalis* is afforded through the pheromone-responsive plasmids. The pheromone-responsive plasmids are narrow host range conjugative plasmids that disseminate antibiotic resistance and virulence genes among *E. faecalis* (5, 8-10) and mobilize resistance genes to other pathogens (2, 11-14).

Some *E. faecalis* encode CRISPR-Cas systems. We have demonstrated that these systems reduce the spread of antibiotic resistance plasmids among *E. faecalis in vitro,* and *in vivo* in the murine intestine (15-19). CRISPR-Cas systems confer sequence-specific genome defense against mobile genetic elements (MGEs) (20, 21). Type II CRISPR-Cas systems occur in *E. faecalis* (22-24). They consist of a CRISPR array and CRISPR-associated (*cas*) genes. In *E. faecalis*, the CRISPR is an array of 36 base pair (bp) repeat sequences interspersed by 30 bp sequences referred to as spacers. When cells are challenged with a MGE, some incorporate a short segment (protospacer) of the invading MGE genome into the CRISPR as a novel spacer (20, 25). By this mechanism, the CRISPR serves as a heritable molecular memory of MGE encounters. Short sequence motifs adjacent to protospacers, called protospacer adjacent motifs (PAMs), as well as the Cas9, Cas1, and Cas2 nucleases are important for adaptation (26-31). The CRISPR is transcribed and processed into small RNAs called crRNAs; one crRNA corresponds to one spacer (32). If a MGE possessing the protospacer and PAM enters the cell, the Cas9 nuclease is directed to the MGE genome by the crRNA. Cas9 cleaves the invading MGE, generating a double-stranded DNA break, thereby inhibiting its entry (33-36).

61

62 Several of our studies (17, 18, 37) have focused on the CRISPR3-Cas locus of the *E. faecalis*
63 strain T11RF, which natively lacks horizontally acquired antibiotic resistance genes (38, 39). *E.*
64 *faecalis* T11RF is closely related to the model multidrug-resistant *E. faecalis* strain V583, but lacks
65 the ~620 kb of horizontally acquired genome content that V583 possesses (39). T11RF has a
66 CRISPR-Cas system, while V583 does not (24). In general, multidrug-resistant *E. faecalis* lack
67 CRISPR-Cas. The *E. faecalis* T11RF CRISPR3-Cas possesses 21 spacers. Spacer 6 is identical
68 to the *repB* gene of the model pheromone-responsive plasmid pAD1. pAD1 encodes a haemolytic
69 bacteriocin referred to as cytolysin and the virulence factor aggregation substance (8, 40). We
70 previously demonstrated that T11RF CRISPR3-Cas interferes with acquisition of the pAD1
71 derivative pAM714, which encodes erythromycin resistance via *ermB* on Tn*917* (41, 42). Deletion
72 of *cas9* or spacer 6 in *E. faecalis* T11RF resulted in up to a 150-fold increase in pAM714
73 acquisition in *in vitro* mating with *E. faecalis* OG1SSp(pAM714) donors (17). This increase in
74 conjugation frequency was not observed for the pheromone-responsive plasmid pCF10, which is
75 not natively targeted by the T11RF CRISPR3 spacers (17). These experiments confirmed that
76 CRISPR3-Cas is a sequence-specific anti-plasmid defense system in *E. faecalis* T11RF.

77

78 Despite *E. faecalis* T11RF CRISPR3-Cas acting as a barrier to pAM714, up to 10^5
79 T11RF(pAM714) transconjugants still arose in *in vitro* conjugation reactions (17). In this study, we
80 tested the investigated the fate of these transconjugants in serial passage experiments with and
81 without selection for the plasmid.

82

83 **Results**

84 **Serial passage experiments to study transconjugant evolution over time.** We mated *E.*
85 *faecalis* OG1SSp(pAM714) donors and T11RF or T11RF Δ*cas9* recipients for 18 hours on agar
86 plates without erythromycin selection (17). After 18 hours, mating reactions were recovered and

87 plated on agar selective for transconjugants, donors, and recipients. These data were previously
88 reported and demonstrated that CRISPR-Cas significantly reduces pAM714 acquisition by T11RF
89 (17). We randomly selected 6 T11RF(pAM714) and 6 T11RFΔ*cas9*(pAM714) transconjugants for
90 further analysis in this study. The 6 T11RF(pAM714) transconjugants are referred to hereafter as
91 WT1-WT6, and the 6 T11RFΔ*cas9*(pAM714) transconjugants are referred to as Δ1-Δ6. The
92 transconjugant colonies were each resuspended in brain heart infusion (BHI) broth. Samples were
93 removed from the colony resuspensions for serial dilution and plating to determine the percentage
94 of erythromycin-resistant cells, and for PCR and sequencing to determine the size and sequence
95 of the CRISPR3. These data are referred to as "Day 0." Next, each transconjugant colony
96 resuspension was split equally into BHI broth and BHI broth with erythromycin and passaged daily
97 for 14 days. At every passage, broth samples were removed to determine the percentage of
98 erythromycin-resistant cells and the size (by agarose gel electrophoresis) and sequence (by
99 Illumina sequencing) of the CRISPR3 amplicon. As a control, wild-type T11RF was also passaged
100 for 14 days in BHI broth.
101
102 At Day 0, the WT1-WT6 populations, except for WT4, were a mix of erythromycin-sensitive
103 (primarily) and erythromycin-resistant cells (Figure S1A). The Δ1-Δ6 populations were comprised
104 of erythromycin-resistant cells (Figure S1A). The CRISPR3 arrays of all populations were wild-
105 type size (1.76 kb) based on PCR amplification and agarose gel electrophoresis analysis of
106 products (Figure S1B).
107
108 **Erythromycin resistance is lost from most WT but no Δ*cas9* populations during passage**
109 **in non-selective medium.** The frequency of erythromycin-resistant cells decreased in the WT1,
110 WT2, WT3, WT5, and WT6 populations over the course of serial passage in BHI broth lacking
111 erythromycin (Figure 1A). In contrast, erythromycin resistance was stably maintained at high
112 frequencies in the WT4 population and all of the Δ1-Δ6 populations in the absence of erythromycin

113 selection (Figure 1A). The CRISPR3 arrays of all populations were of wild-type size based on
114 PCR amplification and agarose gel electrophoresis analysis of products (Figure 1B and Figure
115 S2).
116
117 We analyzed the WT4 population further because it was an outlier compared to the other WT
118 populations. We sequenced the *cas9* coding region of the WT4 population from Day 0 and
119 identified a mutation resulting in an Ala749Thr substitution. Ala749 occurs within the RuvC
120 nuclease domain and is conserved in the well-studied Cas9 of *Streptococcus pyogenes* (17). The
121 Ala749Thr substitution may result in loss in Cas9 function, causing WT4 to phenocopy the Δ1-Δ6
122 populations.
123
124 **CRISPR-Cas mutants emerge in WT populations during passage with erythromycin.** We
125 observed stable maintenance of erythromycin resistance in all WT1-WT6 and Δ1-Δ6 populations
126 during passage with erythromycin selection (Figure 1A). By Day 14 of passage with erythromycin,
127 CRISPR3 arrays in all WT populations except WT1 and WT4 were smaller in size than the wild-
128 type T11RF control (Figure 1B). The variation in array size initiated sporadically over the 14 days,
129 and each transconjugant had a unique pattern (Figure S2). Sanger sequencing of the CRISPR3
130 array amplicons from Day 1 and Day 14 erythromycin-passaged populations revealed that the
131 CRISPR3 spacer 6 was either deleted from the array or the spacer 6 region had poor sequence
132 quality (Table 2). We will refer to spacer 6 as S_6 hereafter, and use this subscript nomenclature
133 for the other 20 spacers of the T11RF CRISPR3 array (e.g., S_1, S_2, etc.).
134
135 In contrast to WT populations, CRISPR3 array sizes for the Δ1-Δ6 populations were unchanged
136 after passage in medium with erythromycin (Figure 1B and Table 2). We chose the Δ4 population
137 as a representative of the Δ1-Δ6 populations for future analyses.
138

139 To investigate whether mutations were present outside the CRISPR3 array, we performed whole
140 genome Illumina sequencing on select populations. We observed variation in the *cas9* sequence
141 of the WT1, WT2, and WT3 Day 14 populations relative to the T11RF wild-type (Table 3). All of
142 the mutations led to nonsynonymous changes (Table 3). Some of the sequenced populations
143 possessed variations in one or more additional genes (Table S2). No mutations were identified in
144 the S_6 protospacer or the PAM region of the *repB* gene in pAM714. However, we did identify a
145 mutation within *repB*, not associated with the protospacer or PAM, in the WT2 population (Table
146 S2). We observed no evidence of Tn*917* movement from pAM714 into the T11 chromosome as
147 all reads overlapping the ends of Tn*917* also overlapped the pAD1 reference sequence.
148
149 **CRISPR3 alleles with spacer deletions are present in most WT populations after serial**
150 **passage with erythromycin selection.** To attain greater resolution of CRISPR3 alleles, we used
151 Illumina sequencing to analyze CRISPR3 amplicons. We analyzed the CRISPR3 amplicons
152 obtained for the WT1-WT6 and Δ4 populations after Day 1 and Day 14 of serial passage with
153 erythromycin. We also analyzed the wild-type T11RF control passaged in BHI broth. We achieved
154 an average of 16 million reads for our amplicons (Table S3).
155
156 To identify specific CRISPR3 alleles in the amplicon sequencing, we created a pool of references
157 by sliding a contiguous and non-overlapping window of 96 bp in length along CRISPR3 reference,
158 which allows each reference to contain exactly two adjacent spacers connected by one repeat.
159 The sliding window starts at 30 bp upstream of the first repeat and ends at 30 bp downstream of
160 the terminal repeat. In total, 22 references were generated to represent wild type alleles. Then,
161 we manually constructed artificial CRISPR3 reference sequences for every possible spacer
162 deletion and rearrangement event with a length of 96 bp. In total, 462 references were constructed
163 to represent all mutant alleles. We then mapped CRISPR amplicon reads to wild-type and mutant
164 references (see Figure S3). The mapping was performed with stringency to allow unique mapping

165 only. After mapping, the number of mapped reads per 96-bp reference was calculated and
166 normalized by the total number of mapped reads per all references. To further evaluate the
167 normalized reads per reference, we calculated z-score using mean and standard deviation from
168 the T11RF Day 1 and Day 14 mapping result. The higher the z-score, the more abundant reads
169 per reference. The significance of z-score was calculated using t-test with a degree of freedom of
170 483. By applying a p-value cutoff of 0.05, we identified the most abundant CRISPR3 alleles in
171 each population (Figure 2 and Table 2). Of the five T11RF transconjugant populations analyzed,
172 all other than WT1 possessed at least one significantly enriched mutant CRISPR3 allele after 14
173 days of passage with antibiotic selection, and each of those alleles lacked S_6 (Table 2).
174
175 One drawback for our method is that it is difficult to set a p-value cutoff. Here we used canonical
176 definition of 0.05. However, the normalized reads per reference for wild-type alleles is expected
177 to be much higher than that from mutant alleles, and in fact, it is much higher in control samples
178 (T11RF control Day 1 and Day 14). Such variation results in large standard deviation values which
179 skew the calculation of z-scores and hence underestimates the abundance of mutant alleles. We
180 predict that more mutant alleles existed in Day 14 WT transconjugant samples, which is supported
181 by an examination of the normalized reads per reference plot (Figure S4), but we are uncertain
182 about their significance as measured by p-value. Supporting our approach, control samples
183 yielded results largely as expected. In control samples (T11RF and the representative Δ*cas9*
184 transconjugant), only wild type alleles were significantly abundant with p-value < 0.05. However,
185 we also observed uneven distribution among different 96-bp references representing wild-type
186 alleles, which resulted in a "loss of spacer16-17" call for the Day 14 Δ*cas9* transconjugant at the
187 p-value of 0.057. When looking at the normalized reads per reference heatmap (Figure S4), we
188 believe spacer16-17 was still largely intact within the Δ*cas9* transconjugant population, the
189 abundance of which is about 1000 times more than that from a mutant 96-bp reference. In short,
190 our statistical approach has strengths and weaknesses, which have been discussed here.

191

192 **Functional assays confirm that CRISPR-Cas defense was compromised after antibiotic**
193 **selection.** Our sequencing analyses suggested that the WT transconjugants passaged with
194 erythromycin had become deficient for CRISPR-Cas defense either by deletion of spacer 6 or
195 inactivation of Cas9 by mutation. For a functional assessment, we tested whether the
196 transconjugant populations could still defend against sequences targeted by T11RF CRISPR3-
197 Cas. To do this, we utilized the pheromone-responsive plasmid pCF10 (43), which is not natively
198 targeted by the T11RF CRISPR3-Cas system. We previously demonstrated that pCF10 transfer
199 into wild-type and Δ*cas9* T11RF strains is equivalent (17). In this study, we modified pCF10 to be
200 targeted by the T11RF CRISPR3-Cas system. We generated three derivatives of *E. faecalis*
201 OG1SSp(pCF10), each with an insertion of a T11RF CRISPR3 spacer (S_1, S_6, or S_7) and
202 CRISPR3 consensus PAM in the pCF10 *uvrB* gene (Figure 3A). Disruption of *uvrB* does not
203 impact pCF10 conjugation (17). We then compared conjugation of wild-type pCF10 and these
204 derivatives into the control T11RF population that had been passaged in BHI broth for 14 days.
205 As expected, conjugation frequencies were significantly lower for all pCF10 derivatives bearing
206 CRISPR3 targets, as compared to the wild-type pCF10 (Figure 3B).

207

208 We then evaluated pCF10 transfer into the WT5 Day 14 populations. For WT5 passaged without
209 erythromycin, we observed similar results to the T11RF control (Figure 3B), demonstrating that
210 the CRISPR3-Cas system in this population is still functional. For WT5 passaged with
211 erythromycin, conjugation frequency of only the pCF10 derivative bearing S_1 was reduced relative
212 to wild-type pCF10 (Figure 3B). This is consistent with the deletion of S_6 and S_7 in this population
213 (Figure 2), and demonstrates that the sequencing data are accurate and not the result of PCR
214 amplification bias. We note that we observed a ~3 log higher conjugation frequency of pCF10 into
215 this population compared to the WT5 population passaged without erythromycin (Figure 3B). This
216 is due to comparatively low donor numbers (averages of 7.1×10^6 and 5.6×10^9 CFU/mL,

217 respectively; raw transconjugant and donor numbers for Figure 2 are presented in Dataset S1).
218 pAM714 encodes the bacteriocin, cytolysin (8). We previously reported that *E. faecalis* with
219 pAM714 kill *E. faecalis* cells that lack pAM714 (18). The probable explanation is that the WT5
220 population passaged with erythromycin, which has a very high carriage rate of pAM714 (Figure
221 1) killed OG1SSp(pCF10) donors using cytolysin.
222
223 We also evaluated pCF10 transfer into the WT4 Day 14 populations. WT4 was unique among the
224 6 WT transconjugants in that it maintained erythromycin resistance at high frequencies in the
225 absence of erythromycin selection (Figure 1A). We identified a probable loss-of-function mutation
226 in the RuvC domain-encoding region of *cas9*. The WT4 populations did not interfere with any of
227 the three pCF10 derivatives bearing CRISPR3 targets (Figure 3B). This is consistent with a loss
228 of CRISPR-Cas function in the WT4 populations conferred by a loss of function mutation in *cas9*.
229
230 **Analysis of *E. faecalis* genomes identifies a strongly supported instance of *in situ* CRISPR-**
231 **Cas compromise.** Our data demonstrate that loss-of-function mutations in CRISPR-Cas arise
232 that promote plasmid acquisition (for WT4) or plasmid maintenance (for WT2-3 and WT5-6) in *E.*
233 *faecalis*. We used genome data available for *E. faecalis* to identify potential instances where this
234 may have occurred in nature. We focused on published MDR *E. faecalis* strains that possess
235 CRISPR-Cas, reasoning that CRISPR-Cas function may have been compromised, allowing for
236 the accumulation of acquired resistance genes. More specifically, we narrowed our focus to
237 strains that both encode CRISPR-Cas as well as resistance to the last-line antibiotics vancomycin
238 or linezolid, which are often plasmid-borne. Using these strict criteria, we analyzed the literature
239 and identified one strongly supported occurrence of CRISPR-Cas compromise. The MDR *E.*
240 *faecalis* strain KUB3006, for which a completely closed genome is available (44), possesses 4
241 plasmids, including one that encodes linezolid resistance. Yet, it also encodes CRISPR3-Cas
242 (44). The *cas9* gene is frameshifted, and the frameshift occurs within the codon for one of the two

243 Cas9 active sites that we previously experimentally confirmed in *E. faecalis* (17). We conclude
244 that CRISPR3-Cas function is likely to be compromised in this strain, which requires experimental
245 confirmation.
246
247 **Discussion**
248
249 In this study we investigated the fates of *E. faecalis* transconjugants that acquired a CRISPR-
250 targeted plasmid, using serial passage with and without antibiotic selection for the plasmid.
251
252 We observed that 5 of 6 wild-type T11RF(pAM714) transconjugants lost the plasmid over the
253 course of antibiotic-free serial passage, while T11RFΔ*cas9*(pAM714) transconjugants maintained
254 the plasmid. This is indicative of active CRISPR-Cas defense in the T11RF(pAM714)
255 transconjugant populations. An important caveat is that erythromycin is a bacteriostatic antibiotic,
256 and we did not restreak transconjugant colonies before starting the serial passage experiment,
257 therefore we cannot be certain that plasmid-free T11RF surviving on the transconjugant selective
258 agar were not carried over with the initial transconjugant colonies that were picked. At least two
259 non-mutually exclusive explanations for our observations are possible. The first is that T11RF
260 cells lacking pAM714 (either carried over or sporadically arising) outcompete T11RF(pAM714)
261 cells. This competitive effect is due to the growth defect of cells that simultaneously possess
262 CRISPR-Cas and one of its plasmid targets, as we have previously reported (15, 16). The second
263 is that CRISPR-Cas 'scrubs' pAM714 from T11RF over the course of antibiotic-free serial
264 passage. We point to Figure S1, where the WT4 colony stands out as containing essentially all
265 erythromycin-resistant cells, while the other WT transconjugant colonies do not. As determined in
266 this study, WT4 is a *cas9* loss-of-function mutant. These results seem to favor the second
267 explanation, since carryover of erythromycin-sensitive cells may have equally affected the
268 randomly selected WT4 colony compared to other randomly selected WT colonies. Regardless,

269 this could be further investigated by repeating the experiment and streaking the initial
270 transconjugant colonies prior to serial passage.
271
272 On the other hand, when the same T11RF(pAM714) transconjugants were passaged with
273 antibiotic selection, the plasmid was maintained, as expected, but variants emerged that lacked
274 the spacer targeting the plasmid. In some cases, multiple sequential spacers were deleted, and
275 we demonstrated that this resulted in loss of defense against multiple plasmids (specifically,
276 pAM714 and derivatives of pCF10; see WT5, Fig. 3). This supports our CRISPR amplicon
277 sequence analysis by demonstrating that spacer losses identified by sequencing corresponded
278 with loss of functional CRISPR-Cas defense. Variations in *cas9* were also observed in some
279 antibiotic-passaged populations, but not experimentally investigated, so their impacts on
280 CRISPR-Cas function remain undefined. We also identified one very strongly supported example
281 of CRISPR-Cas compromise in an independent *E. faecalis* isolate (KUB3006) with a closed
282 genome. Other studies have identified spacer deletion events occurring in transformants or
283 transconjugants of CRISPR-targeted plasmids (45-47) providing more evidence that loss-of-
284 function mutations in CRISPR-Cas contribute to antibiotic resistance plasmid dissemination in
285 bacterial populations.
286
287 Our work occurs in the broader context of work on “self-targeting” spacers in CRISPR-Cas
288 systems, which have been studied for some time across different types of CRISPR-Cas in
289 different species (48). Self-targeting spacers typically refer to those with sequence
290 complementarity to targets within the host genome. This phenomenon was mostly observed
291 during phage infection and plasmid invasion (49), but self-targeting spacers against non-mobile
292 elements have also been reported (50). Different hypotheses have been posited for their
293 maintenance in microbial genomes, including alteration of target sites via DNA repair (51-53),
294 large deletion of the target sites (54), alteration of the PAM sequence (55), loss of spacers (16,

295 56) or mutations in *cas* genes (54). The “self-targeting” outcome is dependent on the fitness cost
296 and environmental selective pressure (57). The conflict between active CRISPR-Cas and “self-
297 targeting” spacers plays a role in shaping bacterial evolution, including altering the population-
298 level genetic diversity (58-60), remodeling of pathogenicity islands (61) and modulation of
299 metabolic pathways (62). Our work sought to investigate how this conflict can be resolved in *E.*
300 *faecalis*, as entry and maintenance of pAM714 into wild-type T11RF creates a “self-targeting”
301 situation that theoretically must be resolved to prevent persistent stress from DNA damage at the
302 targeted pAM714 *repB* site. In essence, this is the basis of CRISPR-Cas gene editing, and in a
303 previous study we took advantage of this property to implement CRISPR-Cas9 gene editing in *E.*
304 *faecalis* (15). Here, a recombination template to repair DNA damage (in this case, damage to
305 pAM714 *repB*) was not provided to the cells. We observed (in general) that the “self-targeting”
306 CRISPR spacer was retained and the target lost in populations passaged without antibiotic
307 selection for the target. On the other hand, CRISPR spacer and/or potentially overall CRISPR-
308 Cas function was lost, and the target retained, in populations passaged with antibiotic selection
309 for the target. In other studies, these “self-targeting” spacers have been engineered to promote
310 the loss of genomic islands and other mobile elements in bacteria (54, 61, 63). Our results
311 demonstrate that selection for the targeted element impedes this process, which is relevant to the
312 design and implementation of CRISPR-based antimicrobials that “cure” *E. faecalis* of antibiotic
313 resistance genes (19, 64). Our results suggest that these systems will need to be introduced and
314 utilized either pre- or post-antibiotic therapy, not during.
315
316 Overall, we posit that the interplay of CRISPR-Cas, plasmids, and antibiotic selection should be
317 further investigated to understand the role of CRISPR-Cas in the antibiotic resistance crisis.
318 Particularly important will be experimental designs that better replicate the *in vivo* setting where
319 antibiotic resistance plasmids disseminate, for e.g., the gastrointestinal tract, where multispecies
320 biofilms are present, and cell densities, mutation rates, CRISPR-Cas activities, and antibiotic

321 concentrations are likely to vary. More specifically, it remains unclear how frequently CRISPR-
322 Cas spacer deletion or loss-of-function mutants arise *in vivo* under antibiotic selection for "self-
323 targeted" plasmids. In a prior study, we assessed the *in vivo* functioning of T11RF CRISPR-Cas
324 against pAM714 in a mouse intestinal colonization model where OG1SSp(pAM714) donors and
325 T11RF or T11RFΔ*cas9* recipients were introduced (18). CRISPR-Cas defense against pAM714
326 appeared robust – no T11RF(pAM714) transconjugants stably colonized the mouse intestine
327 above our limit of detection (<10^2 CFU/g feces). Conversely, T11RFΔ*cas9*(pAM714)
328 transconjugants were stably present in most mice (up to ~10^7 CFU/g feces). The key question we
329 did not answer in that study is whether T11RF(pAM714) transconjugants with spacer 6 deletions
330 or other loss-of-function mutations in CRISPR-Cas would have emerged if we had treated the
331 mice with erythromycin. This remains an outstanding question to be addressed.
332
333 **Materials and Methods**
334
335 **Strains, reagents, and routine molecular biology procedures.** Bacterial strains and plasmids
336 used in this study are listed in Table 1. *E. faecalis* strains were grown in Brain Heart Infusion (BHI)
337 broth or on agar plates at 37°C unless otherwise noted. Antibiotics were used for *E. faecalis* at
338 the following concentrations: erythromycin, 50 µg/mL; chloramphenicol, 15 µg/mL; streptomycin,
339 500 µg/mL; spectinomycin, 500 µg/mL; rifampicin, 50 µg/mL; fusidic acid, 25 µg/mL; tetracycline,
340 10 µg/mL. *Escherichia coli* strains used for plasmid propagation and were grown in lysogeny broth
341 (LB) broth or on agar plates at 37°C. Chloramphenicol was used at 15 µg/mL for *E. coli*. PCR was
342 performed using *Taq* (New England Biolabs) or Phusion (Fisher Scientific) polymerases. Primer
343 sequences used are in Table S1. Routine Sanger sequencing was carried out at the
344 Massachusetts General Hospital DNA core facility (Boston, MA). *E. faecalis* electrocompetent
345 cells were made using the lysozyme method as previously described (65).
346

347 **Generation of pCF10 derivatives**. To insert the T11 CRISPR3 spacer 1 (S_1), S_6, and S_7
348 sequences and CRISPR3 PAM (TTGTA) into pCF10, 47 bp and 39 bp single stranded DNA oligos
349 were annealed to each other to generate dsDNA with restriction enzyme overhangs for BamHI
350 and PstI. The annealed oligos were ligated into the pLT06 derivative pWH107 that includes
351 sequence from pCF10 *uvrB*, to insert these sequences into the *uvrB* gene of pCF10 by
352 homologous recombination. A knock-in protocol was performed as previously described (17).
353
354 **Conjugation experiments.** *E. faecalis* donor and recipient strains were grown in BHI overnight
355 to stationary phase. A 1:10 dilution was made for both donor and recipient cultures in fresh BHI
356 broth and incubated for 1.5 hr to reach mid-exponential phase. A mixture of 100 µL donor cells
357 and 900 µL recipient cells was pelleted and plated on non-selective BHI agar to allow conjugation.
358 After 18 h incubation, the conjugation mixture was scraped from the plate using 2 mL 1X PBS
359 supplemented with 2 mM EDTA. Serial dilutions were prepared from the conjugation mixture and
360 plated on BHI agars selective for transconjugants or donors. After 24-48 h incubation, colony
361 forming units per milliliter (CFU/mL) was determined using plates with 30 - 300 colonies. The
362 conjugation frequency was calculated as the CFU/mL of transconjugants divided by the CFU/mL
363 of donors.
364
365 **Serial passage.** Transconjugant colonies were suspended in 50 µL BHI broth. The 50 µL
366 suspension was used as follows: 3 µL was used for PCR to confirm the integrity of the CRISPR
367 array, 10 µL was inoculated into plain BHI broth, another 10 µL was inoculated into selective BHI
368 broth for plasmid selection, and another 10 µL was used for serial dilution and plating on selective
369 medium to enumerate the initial number of plasmid-containing cells in the transconjugant
370 colonies. Broth cultures were incubated for 24 h, followed by 1:1000 dilution into either fresh plain
371 BHI or fresh selective BHI. At each 24 h interval, 3 µL of each culture from the previous incubation
372 was used for PCR to check CRISPR array integrity, and 10 µL was used for serial dilution and

373 plating on agars to determine CFU/mL for total viable cells and plasmid-containing cells. The
374 cultures were passaged in this manner for 14 days; cryopreserved culture stocks were made daily
375 in glycerol. To use the Day 14 transconjugant populations in conjugation reactions, the glycerol
376 stocks were completely thawed on ice, and 20 µL was inoculated into plain BHI broth. The cultures
377 were incubated for 6-8 h to allow them to reach mid-exponential phase (OD_{600nm} ≈ 0.5–0.7), and
378 900 µL was used as recipient in conjugation reactions as described above.
379
380 **Deep sequencing of CRISPR3 amplicons and genomic DNA.** For CRISPR3 amplicon
381 sequencing, 3 µL from a broth culture was used as template in PCR using Phusion Polymerase
382 with CR3_seq_F/R primers (Table S1). The PCR products were purified using the Thermo
383 Scientific PCR purification kit (Thermo Scientific). Genomic DNA was isolated using the phenol-
384 chloroform method (66). The purified PCR amplicons and genomic DNA samples were
385 sequenced using 2 x 150 bp paired end sequencing chemistry by Molecular Research LP (MR
386 DNA; Texas).
387
388 **Whole genome sequencing analysis.** T11 supercontig and pAD1 plasmid contig references
389 were downloaded from NCBI (accession numbers: T11: NZ_GG688637.1-NZ_GG688649; pAD1:
390 AB007844, AF394225, AH011360, L01794, L19532, L37110, M84374, M87836, U00681,
391 X17214, X62657, X62658, M11180 [Tn*917*]). Reads were aligned to these references using
392 default parameters in CLC Genomics Workbench (Qiagen) where ≥50% of each mapped read
393 has ≥80% sequence identity to the reference. Variations occurring with ≥35% frequency at
394 positions with ≥10X coverage between our samples and the reference contigs were detected
395 using the Basic Variant Detector. At the same time, local realignment was performed, followed by
396 Fixed Ploidy variant detection using default parameters and variants probability ≥90% in CLC
397 Genomics Workbench. The basic variants and fixed ploidy variants were combined for each
398 sequencing sample and subjected to manual inspection. The variants that were detected in the

399 T11 genome from all samples were inferred to be variants in our parent T11 stock and were
400 manually removed. The variants that were detected in pAD1 genome from all transconjugant
401 samples were inferred to be variants in our pAM714 stock, hence were also manually removed.
402 Next, variants within the CRISPR3 array were removed as we analyzed CRISPR3 alleles using a
403 different approach (amplicon deep sequencing; see below). All variants detected from all
404 populations were manually checked for coverage depth to eliminate the detection bias. The
405 variants detected in all samples are shown in Table S2. To detect the insertion site of Tn*917*, the
406 mapped reads on reference M11180 were inspected. Reads immediately adjacent to the 5' and
407 3' ends of Tn*917* shared consensus sequences which were later used for blast against T11 and
408 pAD1 (Figure S5). No evidence for Tn*917* insertions other than in the expected position in
409 pAM714 was detected.
410
411 **Analysis of CRISPR3 amplicon sequencing.** To analyze the amplicon sequencing, we first
412 created a pool of references with 96-bp in length to represent both wild type and mutant CRISPR3
413 alleles. In the wild type reference pool, each 96-bp reference contains two adjacent spacers
414 connected by one direct repeat (5'-S_x-R-S_{x+1}-3' where x is from 1 to 20). To include the leader end
415 and terminal end, wild type reference pool also contains 30 bp upstream of the first repeat (S_0)
416 and 30 bp downstream of the terminal repeat (S_T), generating two additional wild type references:
417 5'-S_0-R-S_1-3' and 5'-S_{21}-TR-S_T-3'. In total, 22 references were created to represent wild type
418 CRISPR3 allele.
419
420 To detect CRISPR3 spacer deletions and rearrangements, we manually created an additional
421 462 references with 96-bp in length to represent mutant CRISPR3 alleles. Each mutant reference
422 contains two spacers connected by a direct repeat, where the reference was not already
423 represented in the wild type reference pool. Schematically, the mutant references can be
424 expressed by 5'-spacer[x]-repeat-spacer[y]-3' (5'-S_xRS_y-3') where $y \neq x$. The selection of

425 spacer[x] is from S_0 to S_{21} while the selection of spacer[y] is from S_1 to S_T. Additionally, we assume
426 that if spacer[y] is ST then the repeat would be terminal repeat TR, generating 5'-S_xTRS_T-3' (x is
427 from 0 to 21). In total, 462 references were created with 96-bp in length.
428
429 Sequencing reads were first clipped into 75 bp fragments to enhance mapping efficiency, allowing
430 for retrieval of maximal sequence information. The clipped reads were used to map to the pool of
431 96-bp references using stringent mapping parameters in CLC Genomics Workbench (Qiagen).
432 The stringent mapping parameters require 100% of each mapped read to be ≥95% identical to
433 one unique reference. Thus, the sequencing reads from different CRISPR alleles will be
434 distinguished. The number of mapped reads per each reference was calculated and normalized
435 by the total number of mapped reads to all references, generating normalized reads per reference.
436 The total number of mapped reads to pools of wild type references and mutant references were
437 summarized in Table S3.
438
439 To visualize the normalized reads per reference, a heatmap was generated (Figure S4). On the
440 heatmap, each row name represents 5'-S_x (x is from 0 to 20) and each column name represents
441 R-S_y-3' (y is from 1 to 21) or TR-S_T-3'. The diagonal cells are empty due to the assumption of no
442 repetitive spacers (or 5'-Sx-R-Sx-3'). Intuitively, the cells adjacent to the diagonal cells on the
443 upper side represents wild type pool of references, 5'-Sx-R-Sy-3' where y=x+1 (Figure S3). The
444 cell color represents normalized reads per reference (from white to red to black is lowest to
445 intermediate to the highest abundance).
446
447 To evaluate the statistical significance of normalized mapped reads, we calculated z-score using
448 the mean and standard deviation calculated from T11RF control. Combining the normalized reads
449 per reference from Day 1 and Day 14 T11RF control, we obtained an average normalized reads
450 per reference of 0.002 or 2%) with standard deviation of 0.0096 or 9.6%. These numbers were

451 used to calculated z-score for normalized reads per reference for all samples. To assess the
452 significance, the z-score is further transformed into p-value. A p-value of 0.05 was used as a
453 significant cutoff.
454
455 To visualize the p-value and derive mutant alleles, a heatmap was plotted using the same method
456 as above. The cells with p-value < 0.05 were color coded. To derive the mutant allele, we assume
457 that S_0 and S_T are intact. The sequence of spacers was derived based on the idea of forward
458 algorithm and Viterbi algorithm. Each p-value was considered as a conditional probability: p-value
459 (5'-Sx-R-Sy-3') ~ $P(\text{spacer y} \mid_{\text{spacer x}})$.
460
461 **Accession number.** The sequencing data for amplicon and whole genome sequencing analysis
462 of transconjugant populations has been deposited in the NCBI Sequence Read Archive under
463 PRJNA418345**.**
464
465 **Acknowledgement.** This work was supported by Public Health Service grant R01AI116610 to
466 K.L.P and the Cecil H. and Ida Green Chair to M.Q.Z. We thank Dr. Chen Jia for consultation on
467 data analysis methods.
468
469 **References**
470 1. Lebreton F, Willems RJL, Gilmore MS. 2014. *Enterococcus* Diversity, Origins in Nature,
471 and Gut Colonization. *In* Gilmore MS, Clewell DB, Ike Y, Shankar N (ed), Enterococci:
472 From Commensals to Leading Causes of Drug Resistant Infection, Boston.
473 2. Kristich CJ, Djoric D, Little JL. 2014. Genetic basis for vancomycin-enhanced
474 cephalosporin susceptibility in vancomycin-resistant enterococci revealed using
475 counterselection with dominant-negative thymidylate synthase. Antimicrob Agents
476 Chemother 58:1556-64. 3957902

477 3. Uttley AH, George RC, Naidoo J, Woodford N, Johnson AP, Collins CH, Morrison D,
478 Gilfillan AJ, Fitch LE, Heptonstall J. 1989. High-level vancomycin-resistant enterococci
479 causing hospital infections. Epidemiol Infect 103:173-81. 2249484
480 4. Huycke MM, Sahm DF, Gilmore MS. 1998. Multiple-drug resistant enterococci: the nature
481 of the problem and an agenda for the future. Emerging infectious diseases 4:239.
482 5. Clewell DB, Weaver KE, Dunny GM, Coque TM, Francia MV, Hayes F. 2014.
483 Extrachromosomal and Mobile Elements in Enterococci: Transmission, Maintenance, and
484 Epidemiology. *In* Gilmore MS, Clewell DB, Ike Y, Shankar N (ed), Enterococci: From
485 Commensals to Leading Causes of Drug Resistant Infection, Boston.
486 6. Palmer KL, Kos VN, Gilmore MS. 2010. Horizontal gene transfer and the genomics of
487 enterococcal antibiotic resistance. Curr Opin Microbiol 13:632-9. 2955785
488 7. Hegstad K, Mikalsen T, Coque T, Werner G, Sundsfjord A. 2010. Mobile genetic elements
489 and their contribution to the emergence of antimicrobial resistant *Enterococcus faecalis*
490 and *Enterococcus faecium*. Clinical microbiology and infection 16:541-554.
491 8. Clewell DB. 2007. Properties of *Enterococcus faecalis* plasmid pAD1, a member of a
492 widely disseminated family of pheromone-responding, conjugative, virulence elements
493 encoding cytolysin. Plasmid 58:205-27.
494 9. Dunny GM. 2007. The peptide pheromone-inducible conjugation system of *Enterococcus*
495 *faecalis* plasmid pCF10: cell-cell signalling, gene transfer, complexity and evolution. Philos
496 Trans R Soc Lond B Biol Sci 362:1185-93. 2435581
497 10. Gilmore MS, Segarra RA, Booth MC, Bogie CP, Hall LR, Clewell DB. 1994. Genetic
498 structure of the Enterococcus faecalis plasmid pAD1-encoded cytolytic toxin system and
499 its relationship to lantibiotic determinants. J Bacteriol 176:7335-44. PMC197123
500 11. Jasni AS, Mullany P, Hussain H, Roberts AP. 2010. Demonstration of conjugative
501 transposon (Tn*5397*)-mediated horizontal gene transfer between *Clostridium difficile* and
502 *Enterococcus faecalis*. Antimicrob Agents Chemother 54:4924-6. 2976158
503 12. Showsh SA, De Boever EH, Clewell DB. 2001. Vancomycin Resistance Plasmid in
504 *Enterococcus faecalis* That Encodes Sensitivity to a Sex Pheromone Also Produced by
505 *Staphylococcus aureus*. Antimicrobial Agents and Chemotherapy 45:2177-2178.
506 13. Tsvetkova K, Marvaud JC, Lambert T. 2010. Analysis of the mobilization functions of the
507 vancomycin resistance transposon Tn1549, a member of a new family of conjugative
508 elements. J Bacteriol 192:702-13. 2812457
509 14. Zhu W, Murray PR, Huskins WC, Jernigan JA, McDonald LC, Clark NC, Anderson KF,
510 McDougal LK, Hageman JC, Olsen-Rasmussen M, Frace M, Alangaden GJ, Chenoweth

511 C, Zervos MJ, Robinson-Dunn B, Schreckenberger PC, Reller LB, Rudrik JT, Patel JB.
512 2010. Dissemination of an *Enterococcus* Inc18-Like *vanA* plasmid associated with
513 vancomycin-resistant *Staphylococcus aureus*. Antimicrob Agents Chemother 54:4314-20.
514 2944587
515 15. Hullahalli K, Rodrigues M, Nguyen UT, Palmer K. 2018. An Attenuated CRISPR-Cas
516 System in *Enterococcus faecalis* Permits DNA Acquisition. MBio 9:e00414-18.
517 PMC5930301
518 16. Hullahalli K, Rodrigues M, Palmer KL. 2017. Exploiting CRISPR-Cas to manipulate
519 *Enterococcus faecalis* populations. Elife 6:e26664. PMC5491264
520 17. Price VJ, Huo W, Sharifi A, Palmer KL. 2016. CRISPR-Cas and Restriction-Modification
521 Act Additively against Conjugative Antibiotic Resistance Plasmid Transfer in *Enterococcus*
522 *faecalis*. mSphere 1:e00064-16.
523 18. Price VJ, McBride SW, Hullahalli K, Chatterjee A, Duerkop BA, Palmer KL. 2019.
524 *Enterococcus faecalis* CRISPR-Cas Is a Robust Barrier to Conjugative Antibiotic
525 Resistance Dissemination in the Murine Intestine. mSphere 4:e00464-19. PMC6656873
526 19. Rodrigues M, McBride SW, Hullahalli K, Palmer KL, Duerkop BA. 2019. Conjugative
527 Delivery of CRISPR-Cas9 for the Selective Depletion of Antibiotic-Resistant Enterococci.
528 Antimicrob Agents Chemother 63:e01454-19. PMC6811441
529 20. Barrangou R, Fremaux C, Deveau H, Richards M, Boyaval P, Moineau S, Romero DA,
530 Horvath P. 2007. CRISPR provides acquired resistance against viruses in prokaryotes.
531 Science 315:1709-12.
532 21. Marraffini LA, Sontheimer EJ. 2008. CRISPR interference limits horizontal gene transfer
533 in staphylococci by targeting DNA. Science 322:1843-5. 2695655
534 22. Bourgogne A, Garsin DA, Qin X, Singh KV, Sillanpaa J, Yerrapragada S, Ding Y, Dugan-
535 Rocha S, Buhay C, Shen H, Chen G, Williams G, Muzny D, Maadani A, Fox KA, Gioia J,
536 Chen L, Shang Y, Arias CA, Nallapareddy SR, Zhao M, Prakash VP, Chowdhury S, Jiang
537 H, Gibbs RA, Murray BE, Highlander SK, Weinstock GM. 2008. Large scale variation in
538 *Enterococcus faecalis* illustrated by the genome analysis of strain OG1RF. Genome Biol
539 9:R110. 2530867
540 23. Hullahalli K, Rodrigues M, Schmidt BD, Li X, Bhardwaj P, Palmer KL. 2015. Comparative
541 Analysis of the Orphan CRISPR2 Locus in 242 *Enterococcus faecalis* Strains. PLoS One
542 10:e0138890. 4580645
543 24. Palmer KL, Gilmore MS. 2010. Multidrug-resistant enterococci lack CRISPR-*cas*. MBio 1.
544 2975353

545 25. Garneau JE, Dupuis ME, Villion M, Romero DA, Barrangou R, Boyaval P, Fremaux C,
546 Horvath P, Magadan AH, Moineau S. 2010. The CRISPR/Cas bacterial immune system
547 cleaves bacteriophage and plasmid DNA. Nature 468:67-71.
548 26. Horvath P, Romero DA, Coute-Monvoisin AC, Richards M, Deveau H, Moineau S, Boyaval
549 P, Fremaux C, Barrangou R. 2008. Diversity, activity, and evolution of CRISPR loci in
550 *Streptococcus thermophilus*. J Bacteriol 190:1401-12. 2238196
551 27. Deveau H, Barrangou R, Garneau JE, Labonte J, Fremaux C, Boyaval P, Romero DA,
552 Horvath P, Moineau S. 2008. Phage response to CRISPR-encoded resistance in
553 *Streptococcus thermophilus*. J Bacteriol 190:1390-400. 2238228
554 28. Mojica FJ, Diez-Villasenor C, Garcia-Martinez J, Almendros C. 2009. Short motif
555 sequences determine the targets of the prokaryotic CRISPR defence system.
556 Microbiology 155:733-40.
557 29. Yosef I, Goren MG, Qimron U. 2012. Proteins and DNA elements essential for the CRISPR
558 adaptation process in *Escherichia coli*. Nucleic Acids Res 40:5569-76. 3384332
559 30. Nunez JK, Kranzusch PJ, Noeske J, Wright AV, Davies CW, Doudna JA. 2014. Cas1-
560 Cas2 complex formation mediates spacer acquisition during CRISPR-Cas adaptive
561 immunity. Nat Struct Mol Biol doi:10.1038/nsmb.2820.
562 31. Heler R, Samai P, Modell JW, Weiner C, Goldberg GW, Bikard D, Marraffini LA. 2015.
563 Cas9 specifies functional viral targets during CRISPR–Cas adaptation. Nature 519:199.
564 32. Deltcheva E, Chylinski K, Sharma CM, Gonzales K, Chao Y, Pirzada ZA, Eckert MR, Vogel
565 J, Charpentier E. 2011. CRISPR RNA maturation by trans-encoded small RNA and host
566 factor RNase III. Nature 471:602-7. 3070239
567 33. Jinek M, Jiang F, Taylor DW, Sternberg SH, Kaya E, Ma E, Anders C, Hauer M, Zhou K,
568 Lin S, Kaplan M, Iavarone AT, Charpentier E, Nogales E, Doudna JA. 2014. Structures of
569 Cas9 endonucleases reveal RNA-mediated conformational activation. Science
570 343:1247997.
571 34. Sternberg SH, Redding S, Jinek M, Greene EC, Doudna JA. 2014. DNA interrogation by
572 the CRISPR RNA-guided endonuclease Cas9. Nature 507:62-7.
573 35. Jinek M, Chylinski K, Fonfara I, Hauer M, Doudna JA, Charpentier E. 2012. A
574 programmable dual-RNA-guided DNA endonuclease in adaptive bacterial immunity.
575 Science 337:816-21.
576 36. Gasiunas G, Barrangou R, Horvath P, Siksnys V. 2012. Cas9-crRNA ribonucleoprotein
577 complex mediates specific DNA cleavage for adaptive immunity in bacteria. Proc Natl
578 Acad Sci U S A 109:E2579-86. 3465414

579 37. Huo W, Price VJ, Sharifi A, Zhang MQ, Palmer KL. 2018. *Enterococcus faecalis* strains
580 with compromised CRISPR-Cas defense emerge under antibiotic selection for a CRISPR-
581 targeted plasmid. bioRxiv doi:10.1101/220467:220467.
582 38. McBride SM, Fischetti VA, Leblanc DJ, Moellering RC, Jr., Gilmore MS. 2007. Genetic
583 diversity among *Enterococcus faecalis*. PLoS One 2:e582. 1899230
584 39. Palmer KL, Godfrey P, Griggs A, Kos VN, Zucker J, Desjardins C, Cerqueira G, Gevers
585 D, Walker S, Wortman J, Feldgarden M, Haas B, Birren B, Gilmore MS. 2012.
586 Comparative genomics of enterococci: variation in *Enterococcus faecalis*, clade structure
587 in *E. faecium*, and defining characteristics of *E. gallinarum* and *E. casseliflavus*. MBio
588 3:e00318-11. 3374389
589 40. Weaver KE, Tritle DJ. 1994. Identification and characterization of an *Enterococcus*
590 *faecalis* plasmid pAD1-encoded stability determinant which produces two small RNA
591 molecules necessary for its function. Plasmid 32:168-81.
592 41. Ike Y, Clewell DB, Segarra RA, Gilmore MS. 1990. Genetic analysis of the pAD1
593 hemolysin/bacteriocin determinant in *Enterococcus faecalis*: Tn*917* insertional
594 mutagenesis and cloning. J Bacteriol 172:155-63. 208413
595 42. Clewell DB, Tomich PK, Gawron-Burke MC, Franke AE, Yagi Y, An FY. 1982. Mapping of
596 *Streptococcus faecalis* plasmids pAD1 and pAD2 and studies relating to transposition of
597 Tn*917*. J Bacteriol 152:1220-30. 221629
598 43. Dunny G, Yuhasz M, Ehrenfeld E. 1982. Genetic and physiological analysis of conjugation
599 in Streptococcus faecalis. Journal of bacteriology 151:855-859.
600 44. Kuroda M, Sekizuka T, Matsui H, Suzuki K, Seki H, Saito M, Hanaki H. 2018. Complete
601 Genome Sequence and Characterization of Linezolid-Resistant *Enterococcus faecalis*
602 Clinical Isolate KUB3006 Carrying a *cfr*(B)-Transposon on Its Chromosome and *optrA*-
603 Plasmid. Front Microbiol 9:2576. PMC6209644
604 45. Jiang W, Maniv I, Arain F, Wang Y, Levin BR, Marraffini LA. 2013. Dealing with the
605 evolutionary downside of CRISPR immunity: bacteria and beneficial plasmids. PLoS
606 Genet 9:e1003844. 3784566
607 46. Rao C, Chin D, Ensminger AW. 2017. Priming in a permissive type I-C CRISPR-Cas
608 system reveals distinct dynamics of spacer acquisition and loss. RNA 23:1525-1538.
609 PMC5602111
610 47. Lopez-Sanchez MJ, Sauvage E, Da Cunha V, Clermont D, Ratsima Hariniaina E,
611 Gonzalez-Zorn B, Poyart C, Rosinski-Chupin I, Glaser P. 2012. The highly dynamic

612 CRISPR1 system of *Streptococcus agalactiae* controls the diversity of its mobilome. Mol
613 Microbiol 85:1057-71.
614 48. Wimmer F, Beisel CL. 2019. CRISPR-Cas Systems and the Paradox of Self-Targeting
615 Spacers. Front Microbiol 10:3078. PMC6990116
616 49. Staals RH, Jackson SA, Biswas A, Brouns SJ, Brown CM, Fineran PC. 2016. Interference-
617 driven spacer acquisition is dominant over naive and primed adaptation in a native
618 CRISPR-Cas system. Nat Commun 7:12853. PMC5059440
619 50. Stern A, Keren L, Wurtzel O, Amitai G, Sorek R. 2010. Self-targeting by CRISPR: gene
620 regulation or autoimmunity? Trends Genet 26:335-40. PMC2910793
621 51. Cui L, Bikard D. 2016. Consequences of Cas9 cleavage in the chromosome of *Escherichia*
622 *coli*. Nucleic Acids Res 44:4243-51. PMC4872102
623 52. Stachler AE, Turgeman-Grott I, Shtifman-Segal E, Allers T, Marchfelder A, Gophna U.
624 2017. High tolerance to self-targeting of the genome by the endogenous CRISPR-Cas
625 system in an archaeon. Nucleic Acids Res 45:5208-5216. PMC5435918
626 53. Xu T, Li Y, Shi Z, Hemme CL, Li Y, Zhu Y, Van Nostrand JD, He Z, Zhou J. 2015. Efficient
627 Genome Editing in *Clostridium cellulolyticum* via CRISPR-Cas9 Nickase. Appl Environ
628 Microbiol 81:4423-31. PMC4475897
629 54. Guan J, Wang W, Sun B. 2017. Chromosomal Targeting by the Type III-A CRISPR-Cas
630 System Can Reshape Genomes in *Staphylococcus aureus*. mSphere 2. PMC5687920
631 55. Dy RL, Pitman AR, Fineran PC. 2013. Chromosomal targeting by CRISPR-Cas systems
632 can contribute to genome plasticity in bacteria. Mob Genet Elements 3:e26831.
633 PMC3827097
634 56. Canez C, Selle K, Goh YJ, Barrangou R. 2019. Outcomes and characterization of
635 chromosomal self-targeting by native CRISPR-Cas systems in *Streptococcus*
636 *thermophilus*. FEMS Microbiol Lett 366.
637 57. Westra ER, Levin BR. 2020. It is unclear how important CRISPR-Cas systems are for
638 protecting natural populations of bacteria against infections by mobile genetic elements.
639 Proc Natl Acad Sci U S A 117:27777-27785. PMC7668106
640 58. Rollie C, Chevallereau A, Watson BNJ, Chyou TY, Fradet O, McLeod I, Fineran PC, Brown
641 CM, Gandon S, Westra ER. 2020. Targeting of temperate phages drives loss of type I
642 CRISPR-Cas systems. Nature doi:10.1038/s41586-020-1936-2.
643 59. van Houte S, Ekroth AK, Broniewski JM, Chabas H, Ashby B, Bondy-Denomy J, Gandon
644 S, Boots M, Paterson S, Buckling A, Westra ER. 2016. The diversity-generating benefits
645 of a prokaryotic adaptive immune system. Nature 532:385-8. PMC4935084

646 60. Watson BNJ, Steens JA, Staals RHJ, Westra ER, van Houte S. 2021. Coevolution
647 between bacterial CRISPR-Cas systems and their bacteriophages. Cell Host Microbe
648 29:715-725.
649 61. Vercoe RB, Chang JT, Dy RL, Taylor C, Gristwood T, Clulow JS, Richter C, Przybilski R,
650 Pitman AR, Fineran PC. 2013. Cytotoxic chromosomal targeting by CRISPR/Cas systems
651 can reshape bacterial genomes and expel or remodel pathogenicity islands. PLoS Genet
652 9:e1003454. PMC3630108
653 62. Aklujkar M, Lovley DR. 2010. Interference with histidyl-tRNA synthetase by a CRISPR
654 spacer sequence as a factor in the evolution of *Pelobacter carbinolicus*. BMC Evol Biol
655 10:230. 2923632
656 63. Selle K, Klaenhammer TR, Barrangou R. 2015. CRISPR-based screening of genomic
657 island excision events in bacteria. Proc Natl Acad Sci U S A 112:8076-81. PMC4491743
658 64. Palacios Araya D, Palmer KL, Duerkop BA. 2021. CRISPR-based antimicrobials to
659 obstruct antibiotic-resistant and pathogenic bacteria. PLoS Pathog 17:e1009672.
660 PMC8266055
661 65. Bae T, Kozlowicz B, Dunny GM. 2002. Two targets in pCF10 DNA for PrgX binding: their
662 role in production of Qa and *prgX* mRNA and in regulation of pheromone-inducible
663 conjugation. J Mol Biol 315:995-1007.
664 66. Manson JM, Keis S, Smith JMB, Cook GM. 2003. A Clonal Lineage of VanA-Type
665 *Enterococcus faecalis* Predominates in Vancomycin-Resistant Enterococci Isolated in
666 New Zealand. Antimicrobial Agents and Chemotherapy 47:204-210.
667 67. Gold OG, Jordan HV, van Houte J. 1975. The prevalence of enterococci in the human
668 mouth and their pathogenicity in animal models. Arch Oral Biol 20:473-7.
669 68. Perez-Casal J, Caparon MG, Scott JR. 1991. Mry, a trans-acting positive regulator of the
670 M protein gene of *Streptococcus pyogenes* with similarity to the receptor proteins of two-
671 component regulatory systems. J Bacteriol 173:2617-24. PMC207828
672

673 **Table 1. Bacterial strains and plasmids used.**
674

Name	Description	Reference
***E. faecalis* strains**		
T11RF	Rifampicin- and fusidic acid-resistant derivative of the human urine isolate T11	(17, 39)
T11RFΔ*cas9*	Derivative of T11RF with *cas9* deleted	(17)
OG1RF	Rifampicin- and fusidic acid-resistant derivative of the human oral isolate OG1	(22, 67)
OG1SSp	Spectinomycin- and streptomycin-resistant derivative of OG1; donor strain for conjugation assays	(41-43)
Plasmids		
pAM714	65 kb PRP encoding erythromycin on Tn*917*, derivative of pAD1	(41)
pCF10	67 kb PRP encoding tetracycline resistance on Tn*925*	(43)
pLZ12	Broad host range shuttle vector encoding chloramphenicol resistance	(68)
pKH12	pLZ12 with *oriT*	(16)
pKHS5	pKH12 with CRISPR2 protospacer S5 and CRISPR1/2 PAM	This study
pKHS96	pKH12 with CRISPR1 protospacer S96 and CRISPR1/2 PAM	(16)
pVP107	pLT06 with T11CR2 protospacer and CRISPR1/2 PAM	(17)
pWH107	pVP107 digested with XbaI/SphI and re-ligated with primers pVP107_ XbaI _For/pVP107_SphI_Rev to remove PstI enzyme site	This study
pWH107.S1	pWH107 with T11CR3 protospacer S1 and CRISPR3 PAM inserted between BamHI/PstI	This study
pWH107.S6	pWH107 with T11CR3 protospacer S6 and CRISPR3 PAM inserted between BamHI/PstI	This study
pWH107.S7	pWH107 with T11CR3 protospacer S10 and CRISPR3 PAM inserted between BamHI/PstI	This study

675

676

677 **Table 2. CRISPR alleles.**
678

Sample name	Day 1 Sanger[c]	Day 14 Sanger[c]	Day 1 Amplicon[d]	Day 14 Amplicon[d]
T11RF control[a]	WT	WT	WT	WT
Δ4[b]	WT	WT	WT	WT
WT1[b]	Poor quality at S_6-S_7	WT	WT	WT
WT2[b]	WT	ΔS_2-S_{11}	WT	ΔS_2-S_{11}
WT3[b]	Poor quality at S_6-S_7	ΔS_5-S_7	WT	ΔS_5-S_7
WT5[b]	Poor quality at S_3-S_8	Poor quality at S_3-S_9	WT	ΔS_5-S_8
WT6[b]	Poor quality at S_1-S_7	Poor quality at S_5-S_6	ΔS_5-S_6	ΔS_6

679 [a]T11RF without pAM714 passaged for 14 days in BHI medium.
680 [b]pAM714 transconjugants passaged for 14 days in BHI medium with erythromycin.
681 [c]CRISPR3 alleles detected by Sanger sequencing.
682 [d]CRISPR3 alleles detected by Illumina amplicon deep sequencing. Abundant alleles with p-value
683 < 0.05 are shown.
684

685

686 **Table 3. Nonsynonymous *cas9* mutations detected by whole genome sequencing.**
687

Position	Ref	Allele	Amino acid change	WT1 Day 14[a]	WT2 Day 14[a]	WT3 Day 14[a]
652983	G	A	Gln506*	31.6% (689x)	ND (590x)	ND (577x)
653184	C	T	Glu439Lys	ND (640x)	ND (536x)	24.2% (594x)
653180	AG	T	Leu440fs	ND (640x)	ND (528x)	23.5% (590x)
654165	G	-	Arg112fs	ND (676x)	48.4% (659x)	ND (772x)

688 [a]Shown are variation frequency and coverage at the indicated nucleotide position on *E. faecalis* T11
689 contig 1.11.
690 ND, not detected.

691

692

693 **Figure Legends**

694

695 **Figure 1. Antibiotic resistance phenotypes and qualitative assessment of CRISPR3**
696 **genotypes in serially passaged transconjugant populations.** a) Erythromycin resistant
697 CFU/mL (expressed as percent of total CFU/mL) remaining in *E. faecalis* populations over the
698 course of passage without (left) and with (right) antibiotic selection. WT transconjugant
699 populations are shown in green or red and Δ*cas9* transconjugant populations are shown in black.
700 b) CRISPR3 amplicon size from early (Day 1) and late (Day 14) passage dates for six WT
701 transconjugant populations and a representative Δ*cas9* transconjugant population (Δ4). The
702 CRISPR3 region was PCR-amplified using aliquots from passaged cultures as template. As a
703 control, T11RF without pAM714 was passaged for 14 days and the CRISPR3 locus amplified
704 (T11RF). P: positive control, T11RF genomic DNA. L: DNA ladder.

705

706 **Figure 2. Detection of mutant CRISPR3 array alleles using amplicon sequencing.** Heat maps
707 show the mutant alleles with significant abundance (p-value <0.05) present at Day 1 and Day 14
708 of T11RF control (a) and antibiotic-passaged transconjugant populations (b-g). Each cell within
709 heatmap represents one of the 484 artificial references where a 5' spacer (rows) is linked with a
710 3' spacer (columns) by a repeat. White cells represent mutant alleles that were not significantly
711 abundant.

712

713 **Figure 3. Experimental confirmation of compromised CRISPR-Cas function in antibiotic-**
714 **passaged WT5 and in WT4.** Day 14 transconjugant populations passaged in BHI and
715 erythromycin (Erm) were used as recipients in conjugation reactions with OG1SSp(pCF10) and
716 derivatives of pCF10. a) Schematic of where the T11 CRSPR3 spacer 1, spacer 6 and spacer 7
717 sequences with corresponding PAM (underlined) were introduced into pCF10. Wild-type pCF10
718 is not natively targeted by T11RF CRISPR3-Cas. b) Conjugation frequency (ratio of

719 transconjugants to donors) from mating reactions. A749T refers to the *cas9* mutation detected in
720 the WT4 population. Statistical significance was determined using a student's t-test; P-values: **
721 ≤ 0.01; *** ≤ 0.001; **** ≤ 0.0001.
722
723

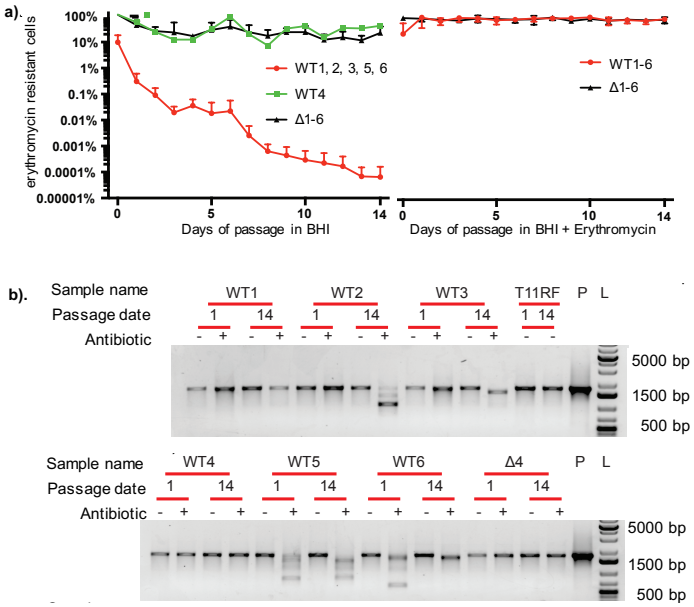
a).
erythromycin resistant cells
100%
10%
1%
0.1%
0.01%
0.001%
0.0001%
0.00001%
WT1, 2, 3, 5, 6
WT4
Δ1-6
WT1-6
Δ1-6
0
5
10
14
Days of passage in BHI
Days of passage in BHI + Erythromycin
b).
Sample name
Passage date
Antibiotic
WT1
WT2
WT3
T11RF
P
L
5000 bp
1500 bp
500 bp
WT4
WT5
WT6
Δ4

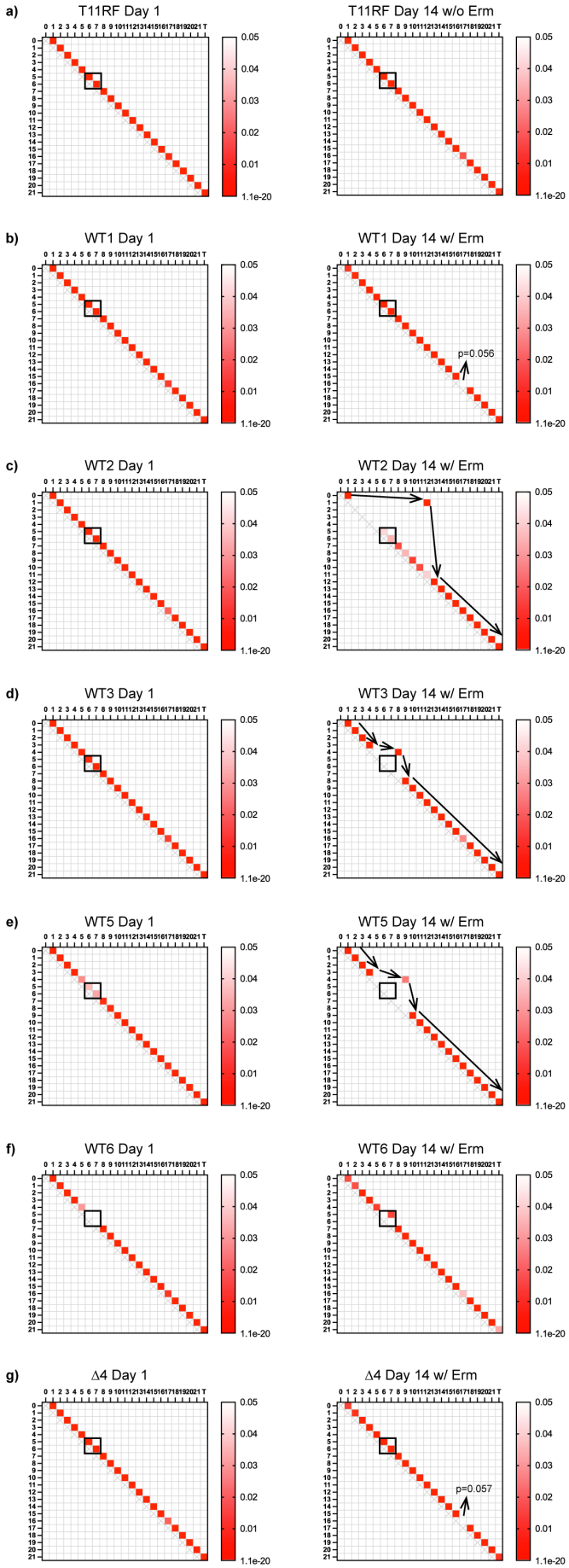
a)
T11RF Day 1
T11RF Day 14 w/o Erm
b)
WT1 Day 1
WT1 Day 14 w/ Erm
p=0.056
c)
WT2 Day 1
WT2 Day 14 w/ Erm
d)
WT3 Day 1
WT3 Day 14 w/ Erm
e)
WT5 Day 1
WT5 Day 14 w/ Erm
f)
WT6 Day 1
WT6 Day 14 w/ Erm
g)
Δ4 Day 1
Δ4 Day 14 w/ Erm
p=0.057
0.05
0.04
0.03
0.02
0.01
1.1e-20

a)

pCF10	WT *uvrB* sequence; not targeted by CRISPR3-*cas*
pCF10+Sp1	AAAAGTTGAATATGTTTCGCTTTGGTGTAATTGTA
pCF10+Sp6	CCGATACAGCTCTTTATTCTTCTAATTACATTGTA
pCF10+Sp7	TGCTTTTGGAGGAATACAAATGAGAAGATTTTGTA

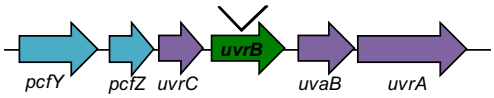

b)

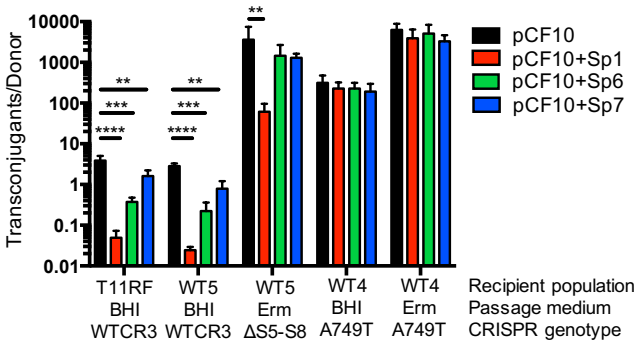

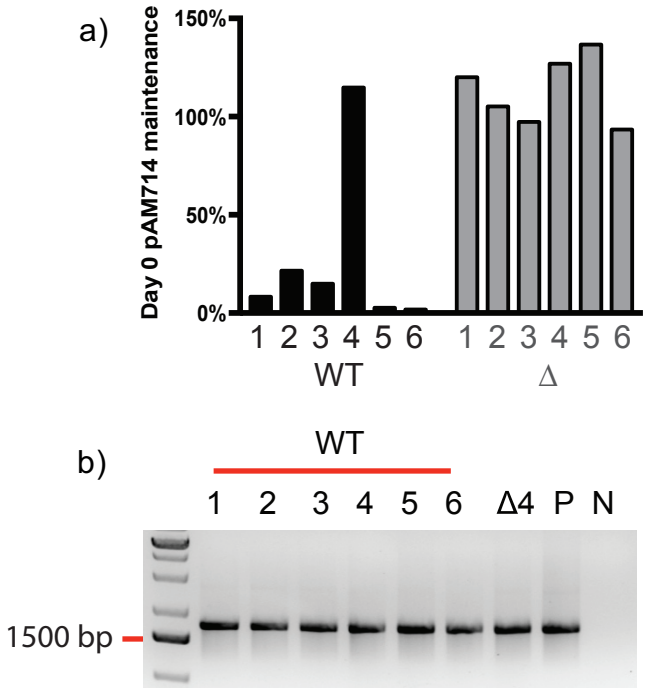

Figure S1. Initial phenotypes of transconjugants chosen for serial passage experiments. a) Frequency of erythromycin resistance in transconjugant colonies used to initiate serial passage experiments. Erythromycin resistance is used to track pAM714 maintenance in the population. b) CRISPR3 amplicon PCR results for transconjugant colonies used to initiate serial passage experiments. Shown are CRISPR3 amplicon sizes for six T11RF pAM714 transconjugants (WT 1-6), a representative T11RFΔ*cas9* pAM714 transconjugant (Δ4), T11RF genomic DNA as a positive control (P), and a reagent control (N).

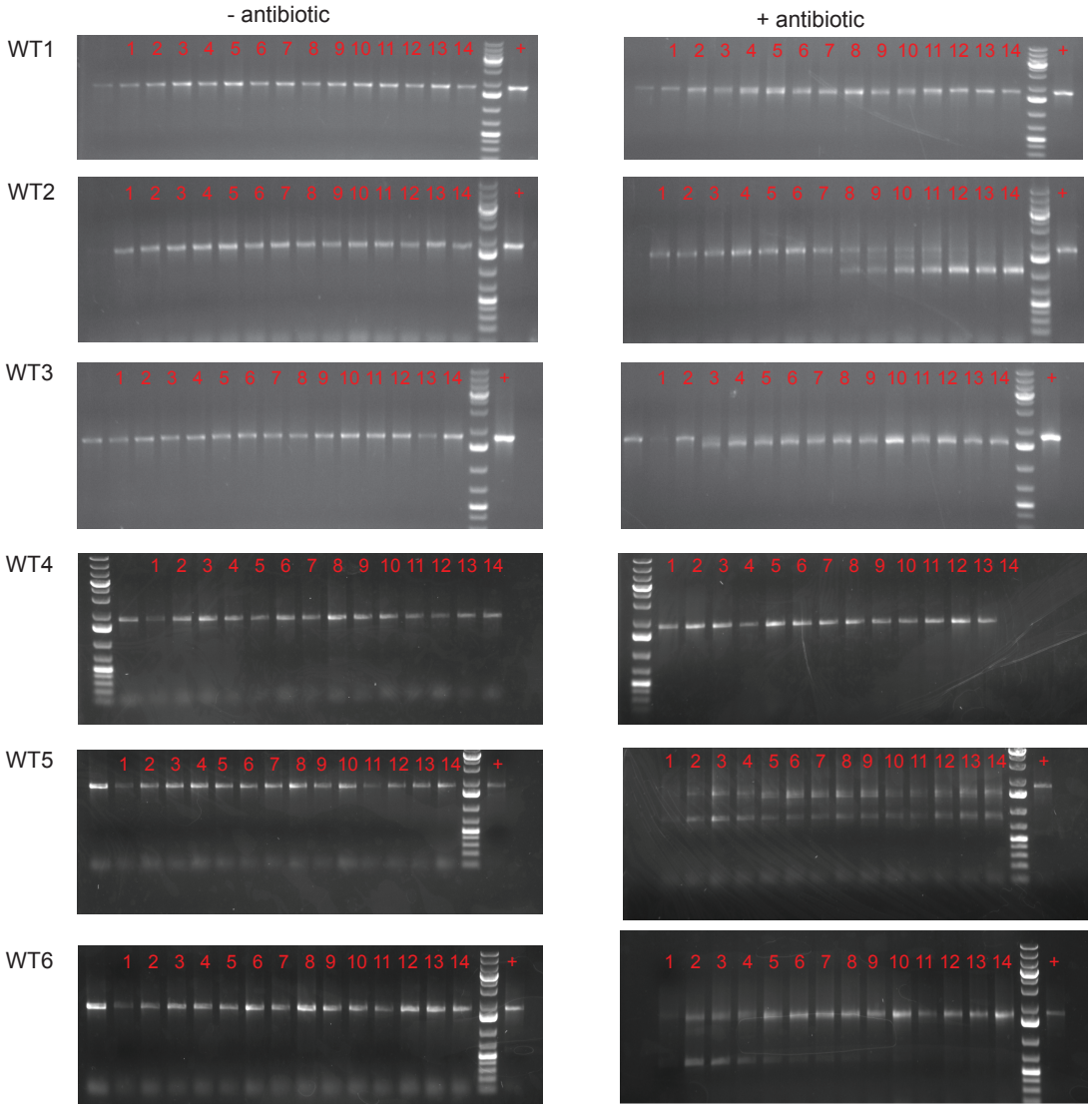

Figure S2. Agarose gel electrophoresis analysis of CRISPR3 amplicons in six T11RF(pAM714) transconjugant populations. Six T11RF(pAM714) transconjugants were serially passaged for 14 days in BHI (left panel) or BHI with erythromycin (right panel). The size of the CRISPR3 array was monitored using PCR and gel electrophoresis on each passage day.

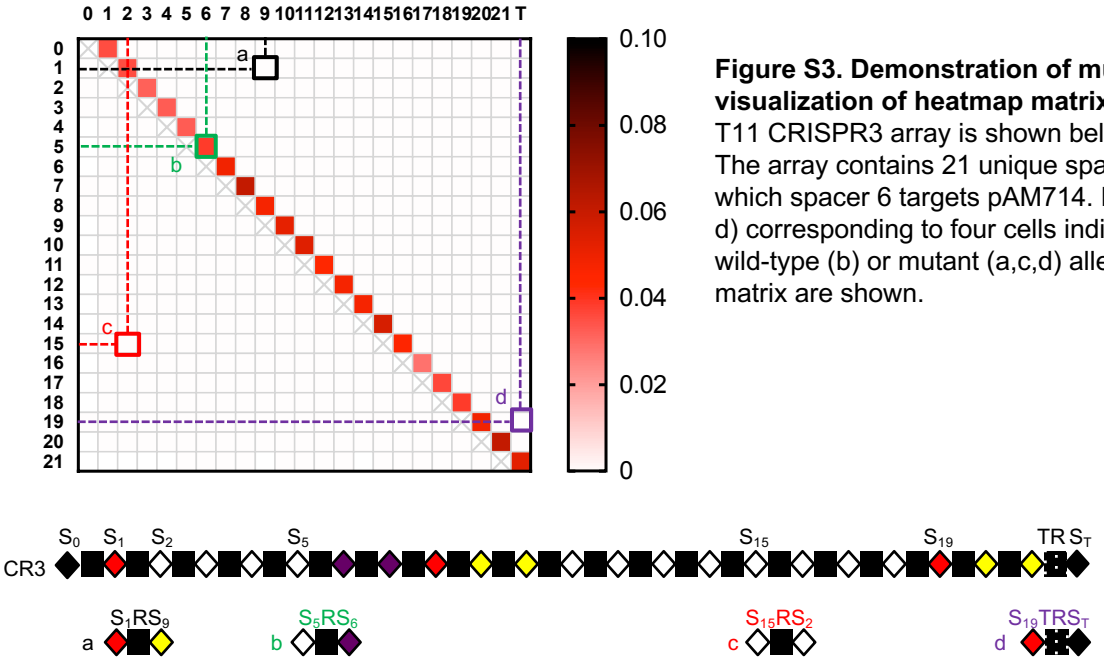

Figure S3. Demonstration of mutant alleles and visualization of heatmap matrix. A cartoon of the T11 CRISPR3 array is shown below the heatmap. The array contains 21 unique spacer sequences, of which spacer 6 targets pAM714. Four scenarios (a-d) corresponding to four cells indicating different wild-type (b) or mutant (a,c,d) allele types in the matrix are shown.

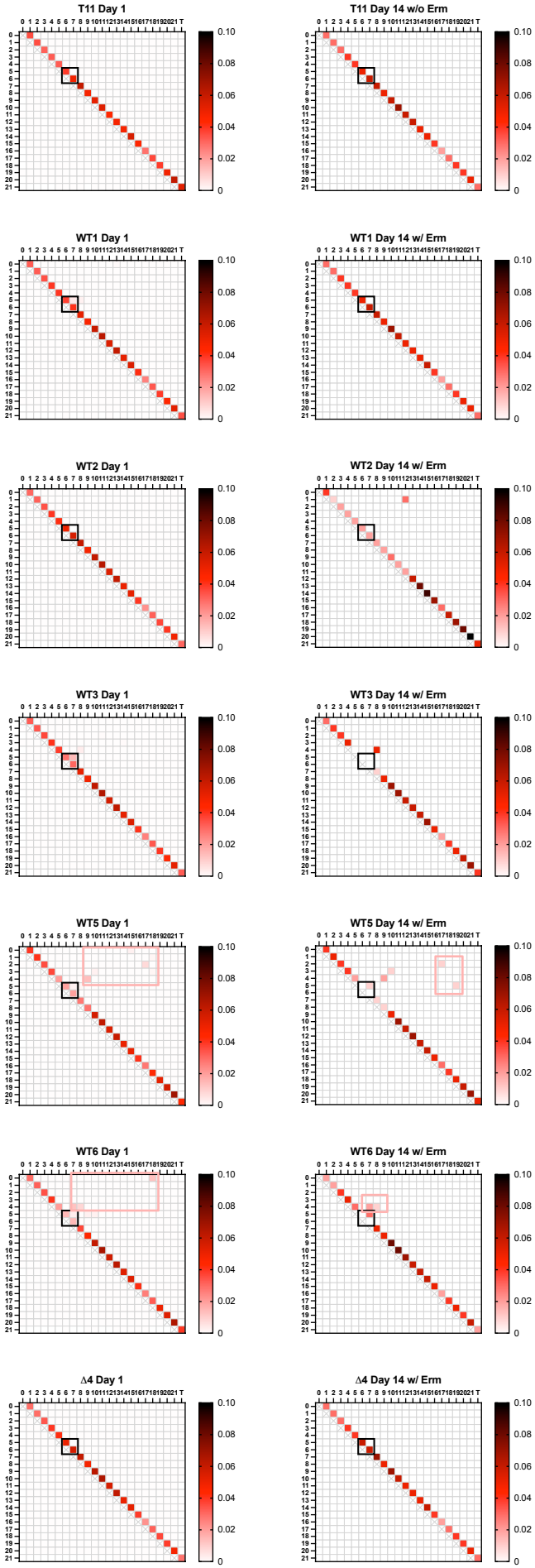

Figure S4. Less abundant mutant alleles can be observed in a heatmap of normalized read counts. Heat maps show the abundance of each mutant allele per sample. Day 1 and Day 14 populations were analyzed and T11RF was used as a control. Each cell within the heat map represents one of the 484 artificial references. The color scale represents low (white) to intermediate (ref) to high (black) abundance alleles. Black boxes indicate the expected wild type allele at the S5-S6 region. Pink boxes surround rare alleles that did not meet the significance cutoff but can be visible here.

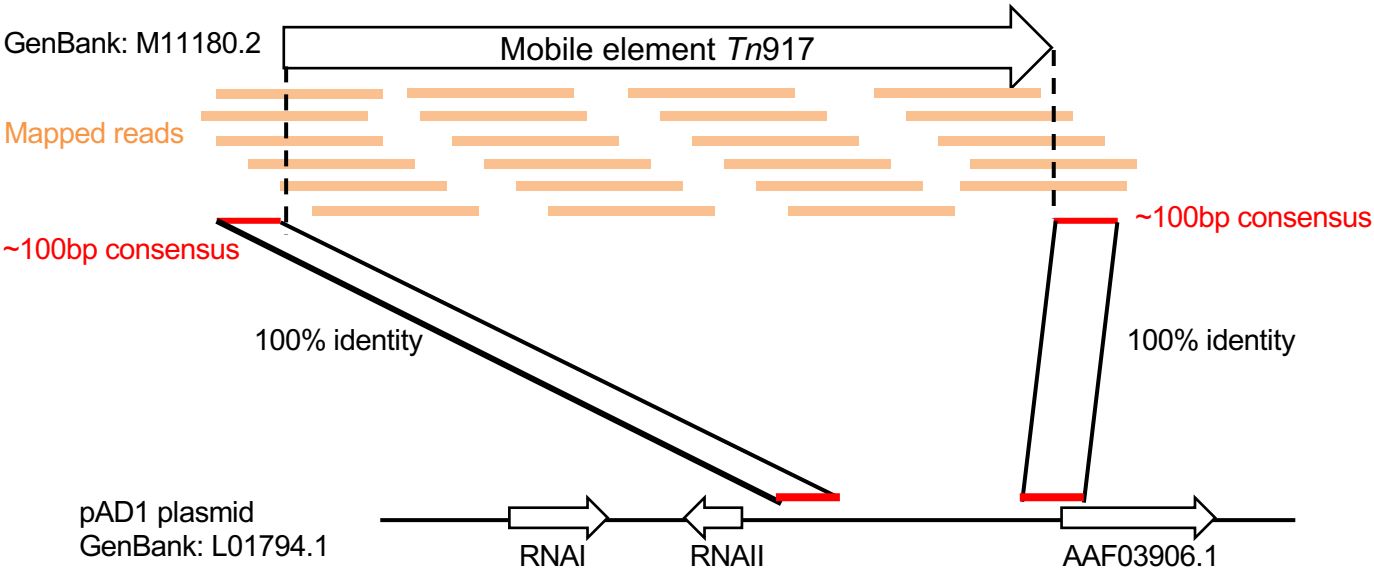

Figure S5. Mapping of Tn*917* location. The consensus sequences were extracted from 5' and 3' ends of transposon Tn*917* and mapped to pAD1 sequences.

Table S1. Primers used in this study.

Name	Primer sequence
CRISPR seq primers	
CRISPR1 seq For	CGTATTTGACAGAGGATGAAG
CRISPR1 seq Rev	CGAATATGCCTGTGGTGAAA
CRISPR2 seq For	TGCTGTTACAGCTACTAAA
CRISPR2 seq Rev	GCCAATGTTACAATATCAAACA
CRISPR3 seq For	GCTCACTGTATTGGAAGAAC
CRISPR3 seq Rev	CATCGATTCATTATTCCTCCAA
pWH107 and derivatives	
pVP107_XbaI_For	CTAGAGATAATATATCTTTTATATAGAAGATGGGTACCATGGCATG
pVP107_SphI_Rev	CCATGGTACCCATCTTCTATATAAAAGATATATTATCT
T11CR3sp6_BamPst_F	GATCCTCCCGATACAGCTCTTTATTCTTCTAATTACATTGTACTGCA
T11CR3sp6_BamPst_R	GTACAATGTAATTAGAAGAATAAAGAGCTGTATCGGGAG
T11CR3sp1_BamPst_F	GATCCTCAAAAGTTGAATATGTTTCGCTTTGGTGTAATTGTACTGCA
T11CR3sp1_BamPst_R	GTACAATTACACCAAAGCGAAACATATTCAACTTTTGAG
T11CR3sp7_BamPst_F	GATCCTCTGCTTTTGGAGGAATACAAATGAGAAGATTTTGTACTGCA
T11CR3sp7_BamPst_R	GTACAAAATCTTCTCATTTGTATTCCTCCAAAAGCAGAG
T11CR2S1 seq arm1 F	CGAAATCAGCACATGGAACA
T11CR2S1 seq arm2 R	CCAGTAACTGTATCAACTAC

Table S2. SNP detection in all genomic DNA sequencing samples.[a]

Contig	Position	Ref	Allele	Annotation	Amino acid change	T11RF[b]	WT3[c]	WT1[d]	WT2[d]	WT3[d]	WT5[d]	WT6[d]	Δ4[d]
AD1REP ABC	1904	C	T	Replication protein	AAB00504.1: p.Pro100Leu				45.49				
1.11	51613	C	T	Collagen adhesin								25.00	
1.11	51674	G	A	Collagen adhesin	WP_002379313.1: p.Gly392Ser						33.90	33.39	
1.11	51745	A	G	Collagen adhesin							33.02		
1.11	337315	G	T	Helicase	WP_002382285.1: p.Glu425*							37.16	
1.11	652983	G	A	Cas9	WP_002379510.1: p.Gln506*			31.64					
1.11	653180	AG	T	Cas9	WP_002379510.1: p.Leu440fs		22.74			23.52			
1.11	653184	C	T	Cas9	WP_002379510.1: p.Glu439Lys		23.21			24.17			
1.11	654165	G	-	Cas9	WP_002379510.1: p.Arg112fs				48.41				
1.11	685523	A	T	Conserved hypothetical protein	WP_002382413.1: p.Glu5Val		23.24						
1.11	685938	A	T	Conserved hypothetical protein	WP_002382413.1: p.Glu143Asp		26.00						
1.11	974866	AT	GC	Cell wall surface anchor family protein	WP_002379620.1: p.Ile972Ala							23.41	
1.11	974991	A	G	Cell wall surface anchor family protein								22.67	
1.2	2903	C	T	Peptidylprolyl isomerase	WP_002355150.1: p.Val167Ile				46.03				

[a] Shown are variation frequencies (%) among the sequencing reads at the indicated nucleotide position relative to *E. faecalis* T11 reference genome.

[b]Day 14 BHI-passaged

[c]Day 1 Erythromycin-passaged population WT3 to confirm presence of *cas9* mutations prior to Day 14

[d]Day 14 Erythromycin-passaged

Table S3. Mapping statistics of the amplicon sequencing.

Sample name	# of Total reads	# mapped to WT pool of references	# mapped to mutant pool of references
Day 1			
T11RF	19,082,652	7,273,291	125,204
Δ4	20,808,404	8,995,910	77,551
WT1	16,736,162	6,808,760	168,051
WT2	16,859,152	7,222,339	59,609
WT3	17,357,970	7,136,664	250,783
WT5	17,744,230	6,784,881	430,500
WT6	16,179,400	6,337,706	406,347
Day 14			
T11RF	17,973,946	7,760,594	68,900
Δ4	14,403,868	5,369,063	55,037
WT1	14,158,158	5,219,558	55,730
WT2	14,538,836	4,489,642	254,615
WT3	17,174,946	5,653,212	385,906
WT5	15,200,646	5,384,356	460,061
WT6	12,325,042	4,201,804	303,973